Letter

Quantum spin liquid in an RKKY-coupled two-impurity Kondo system

Krzysztof P. Wójcik [1,2,3,*] and Johann Kroha [1,†]
[1] *Physikalisches Institut, Universität Bonn, Nussallee 12, D-53115 Bonn, Germany*
[2] *Institute of Molecular Physics, Polish Academy of Sciences, Smoluchowskiego 17, PL-60-179 Poznań, Poland*
[3] *Institute of Physics, Maria Curie-Skłodowska University, PL-20-031 Lublin, Poland*

(Received 23 September 2022; accepted 13 March 2023; published 24 March 2023)

We consider a two-impurity Kondo system with spin-exchange coupling within the conduction band. Our numerical renormalization group calculations show that for strong intraband spin correlations the competition of these nonlocal correlations with local Kondo spin screening stabilizes a phase exhibiting features of a metallic quantum spin liquid, namely nonlocal impurity-spin entanglement and fractionalized charge excitations, without the need for geometric frustration. For weak Kondo coupling, the spin-liquid-like and the Kondo singlet phases are separated by two quantum phase transitions and an intermediate RKKY spin-dimer phase, while beyond a critical coupling they are connected by a crossover. The results suggest how a quantum spin liquid may be realized in heavy-fermion systems with strong magnetic correlations in the conduction band, e.g., near a spin-density-wave instability.

DOI: 10.1103/PhysRevB.107.L121111

Introduction. Quantum spin liquids (QSLs) are systems of interacting spins with long-range entanglement, but without long-range magnetic order down to the lowest observed temperatures. The concept of nonlocal entanglement was first introduced in 1973 by Anderson proposing the resonant valence-bond (RVB) state as the ground state of an antiferromagnetically coupled spin system on a triangular lattice [1], which was later applied to high-temperature cuprate superconductors [2]. Presently, QSLs are a wide and intensive research field in its own right [3–5], due to the possibility of hosting fractional excitations and thus inducing new, unconventional quantum states of matter. Most theoretical studies are done on insulating and geometrically frustrated or topological spin lattice models, such as the triangular, kagome, next-nearest-neighbor coupled, or honeycomb lattices [3–6].

However, some important, possible realizations of QSLs, such as near a magnetic heavy-fermion quantum phase transition (QPT) or in cuprate superconductors [2], require metallic states and are in general not geometrically frustrated. Such systems are generically described by Anderson lattice models, i.e., localized magnetic impurities on a lattice hybridizing with a sea of itinerant conduction electrons. They often exhibit a QPT [7,8] between a paramagnetic heavy Fermi liquid induced by the Kondo effect [9,10] and a magnetically ordered phase due to the Ruderman-Kittel-Kasuya-Yosida (RKKY) spin-spin coupling Y [11–13] mediated by conduction electrons. A QSL in such systems must be stabilized, on the one hand, against the spin extinction due to Kondo singlet formation and, on the other hand, against magnetic ordering. Previous work on metallic, correlated systems predicted a QSL for strong spin-exchange coupling between local and conduction electron spins, but was limited to mean-field treatments [14,15]. Some candidates for metallic QSLs in frustrated Kondo lattices have been proposed [16–20]. However, the existence of metallic QSLs without geometric frustration have remained elusive.

In the present Letter, we study a two-impurity Anderson (2iA) model which incorporates the salient features of correlated Anderson lattice systems, i.e., Kondo singlet formation, a nonlocal spin-exchange (RKKY-like) interaction, and spin correlations within the conduction band, and at the same time is amenable to a numerically exact solution by the numerical renormalization group (NRG) [21–23]. Using NRG calculations we find, in addition to the QPT from a Kondo singlet to a dimer singlet phase at weak RKKY coupling, another QPT at strong coupling from the dimer to another phase, characterized by fractional impurity spectral density and impurity-spin entanglement. We therefore term this phase a two-impurity analog of a bulk QSL. This QSL phase is driven by a dynamical effect, the competition between Kondo screening and strong intraband spin correlations. This phase is continuously connected to the Kondo singlet phase via strong Kondo spin exchange. That is, the Kondo effect stabilizes the QSL against RKKY dimer formation. We discuss potential experimental realizations of this QSL phase and its relevance for metallic lattice spin systems.

Model. Early works by Jones and Varma (JV) [24–26] effectively considered a two-impurity Kondo model where each spin-$1/2$ impurity is coupled to its own metallic host by the Kondo coupling J_{K}, and the RKKY interaction Y is replaced by a direct Heisenberg exchange J_{H} between the two impurities [see Fig. 1(a)]. In this model, the Kondo singlet ground state and a dimer singlet phase, characterized by a $\pi/2$ or 0 scattering phase shift of each impurity, respectively, are separated by a QPT as a function of the control parameter $J_{\mathrm{H}}/T_{\mathrm{K}}^0$, where T_{K}^0 is the Kondo temperature of a single Kondo

*kpwojcik@ifmpan.poznan.pl
†kroha@th.physik.uni-bonn.de

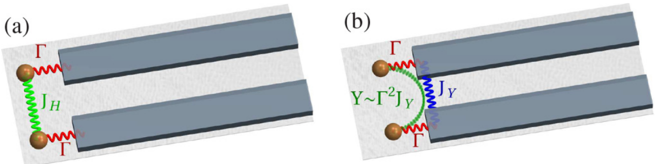

FIG. 1. Illustration of the 2iA model with (a) JV direct spin exchange J_{H} between the impurities and (b) conduction-electron-mediated (RKKY) coupling via the Heisenberg exchange J_Y [Eq. (1)].

impurity [10]. However, any particle-hole (PH) asymmetry of the JV model changes the QPT into a crossover [27,28]. Moreover, it has even been shown that with a proper modeling of the RKKY interaction, the antiferromagnetic contribution to Y stems from the PH-asymmetric component of the effective Hamiltonian [29]. Hence, generically a QPT does not occur in two-impurity systems with one common host [30,31], although the QPT may be restored by a counterterm compensating potential scattering [29], by suppressing charge transfer between the screening channels [32], or by self-consistency in the auxiliary 2iA model in a dynamical mean-field treatment of the lattice [33]. Another difficulty of the JV treatment [24–26] is that, unlike J_{H}, the true RKKY interaction is not independent of the Kondo exchange J_{K}, but rather $Y \sim J_{\mathrm{K}}^2$ [11–13]. This leads to a dynamical frustration effect and a universal suppression of the Kondo scale depending on Y, $T_{\mathrm{K}}^0 \to T_{\mathrm{K}}(Y)$, as has been shown experimentally [34] and theoretically [35]. These problems have called into question the relevance of the JV quantum critical point for QPTs in Kondo and Anderson lattice systems.

Therefore, we consider a maximally symmetric 2iA model with conduction-electron-mediated impurity-spin coupling but without interhost potential scattering as follows [cf. Fig. 1(b)],

$$H_{2\mathrm{iA}} = \sum_{\alpha\mathbf{k}\sigma} \varepsilon_{\mathbf{k}} c^\dagger_{\alpha\mathbf{k}\sigma} c_{\alpha\mathbf{k}\sigma} + \sum_{\alpha\mathbf{k}\sigma} V (c^\dagger_{\alpha\mathbf{k}\sigma} d_{\alpha\sigma} + d^\dagger_{\alpha\sigma} c_{\alpha\mathbf{k}\sigma}) - \frac{U}{2} \sum_{\alpha\sigma} n_{\alpha\sigma} + U \sum_{\alpha} n_{\alpha\uparrow} n_{\alpha\downarrow} + J_Y \vec{s}_1 \cdot \vec{s}_2. \tag{1}$$

Here, $d^\dagger_{\alpha\sigma}$, $d_{\alpha\sigma}$ and $n_{\alpha\sigma} = d^\dagger_{\alpha\sigma} d_{\alpha\sigma}$ are the operators for electrons with spin $\sigma = \uparrow, \downarrow$ on impurity $\alpha = 1, 2$, coupled to their respective conducting leads with operators $c^\dagger_{\alpha\mathbf{k}\sigma}$, $c_{\alpha\mathbf{k}\sigma}$ and dispersion $\varepsilon_{\mathbf{k}}$ by the hybridization V, which we assume to be momentum independent (local) for simplicity. U denotes the on-site repulsion on the impurity sites. Taking $-U/2$ for the impurity single-particle level and a flat conduction electron density of states ρ at the Fermi level ensures PH symmetry. The hybridization generates the Kondo spin-exchange coupling $J_{\mathrm{K}} = 4|V|^2/U$ and the single-particle impurity-level broadening $\Gamma = \pi\rho|V|^2$ [10]. The conduction electron spin at the impurity site of host α is defined in terms of the vector of Pauli matrices $\vec{\sigma}$ and $c_{\alpha\sigma} \equiv \sum_{\mathbf{k}} c_{\alpha\mathbf{k}\sigma}$ as

$$\vec{s}_\alpha = \frac{1}{2} \sum_{\sigma\sigma'} c^\dagger_{\alpha\sigma} \vec{\sigma}_{\sigma\sigma'} c_{\alpha\sigma'}. \tag{2}$$

The last term in the Hamiltonian (1) describes a Heisenberg exchange of strength J_Y between these conduction electron spins. Thus, this model represents a single host as far as spin correlations are concerned. It preserves PH symmetry, there is no symmetry-breaking charge transfer between the leads, and at the same time it generates an RKKY-like coupling between the impurity spins $\vec{S}_\alpha$, mediated by the conducting hosts $Y \vec{S}_1 \cdot \vec{S}_2$, where $Y \approx (\rho J_{\mathrm{K}})^2 J_Y/4$ and $\vec{S}_\alpha$ is defined analogous to Eq. (2). This model captures the salient features of the RKKY interaction, i.e., nonlocality, mediation by the conduction electrons and generation in second order by the Kondo exchange J_{K}, while its power-law dependence on the impurity separation appears irrelevant for the present study. The conduction-mediated coupling Y turns out to be crucial for the phase diagram of the system, while the robustness of the results against the asymmetry effects is discussed in Ref. [36].

We analyze the system using the full density matrix approach to NRG [37,38], which allows for the precise calculation of thermal expectation values and determination of retarded Green's functions $\langle\langle \cdots \rangle\rangle^{\mathrm{ret}}$ directly in their Lehmann representation. We use the open-access code [23] as a basis for our programs, with discretization parameter $\Lambda = 2.5$ and energy cutoff at each iteration $6 < E_{\mathrm{cut}} < 6.5$; see also Ref. [36]. The different phases of the system are characterized by the normalized local spectral density of impurity electrons, $\mathcal{A}_T(\omega) = -\Gamma\, \mathrm{Im}\langle\langle d_{\alpha\sigma}; d^\dagger_{\alpha\sigma}\rangle\rangle^{\mathrm{ret}}(\omega)$, and of conduction electrons at the impurity site, $\mathcal{B}_T(\omega) = -2D\, \mathrm{Im}\langle\langle c_{\alpha\sigma}; c^\dagger_{\alpha\sigma}\rangle\rangle^{\mathrm{ret}}(\omega)$. Equivalently, we will also use the corresponding T-dependent differential conductances, $G(T) = -\int d\omega f'(\omega) A_T(\omega)$ and $g(T) = -\int d\omega f'(\omega) B_T(\omega)$, where $f'(\omega)$ is the ω derivative of the Fermi-Dirac distribution function. We define the single-impurity Kondo scale T_{K}^0 as that temperature where $G(T)$ reaches $1/2$ of its maximum fixed-point value G_0 during the NRG flow (see also below).

Kondo versus Heisenberg quasiparticles. In order to illustrate the competition between Kondo and intraband screening we first recollect two limiting cases of Eq. (1) separately.

(1) $J_{\mathrm{K}} > 0, J_Y = 0$: The single-impurity spin-1/2 Kondo or Anderson model is well understood [9,10,21]. The local spin exchange J_{K} between impurity and host induces the Kondo effect, i.e., the formation of a spatially extended, many-body spin-singlet state comprising the impurity spin and a multitude of conduction electron states for $T < T_{\mathrm{K}}^0$, the Kondo screening cloud [39,40]. This happens for arbitrarily small $J_{\mathrm{K}} > 0$, since J_{K} is subjected to the renormalization group flow toward the strong-coupling fixed point [21]. This ground state is a Fermi liquid, and its excitations are characterized by the Abrikosov-Suhl resonance in the impurity spectral density of unit height, $\mathcal{A}_0(0) = 1$, and width T_{K}^0, the effective bandwidth of the Kondo quasiparticles (QPs). The conduction spectral density at the impurity site $\mathcal{B}_0(\omega)$ is proportional to the inverse QP lifetime and vanishes in a Fermi-liquid manner as $\sim(\omega/T_{\mathrm{K}}^0)^2$.

(2) $J_{\mathrm{K}} = 0$, $J_Y > 0$: An analogous spin screening occurs when two metallic leads are coupled to each other by a Heisenberg interaction J_Y without impurities. This interlead coupling leads to the destruction of free band electrons and the formation of another Fermi-liquid phase, signaled by the low-frequency vanishing of the spectral density at the coupled sites as $\mathcal{B}_0(\omega) \sim (\omega/D)^2$. However, unlike in the Kondo case, this happens only above a critical coupling strength, $J_Y > J_Y^{**}$, since J_Y is not renormalized to a strong-coupling fixed point

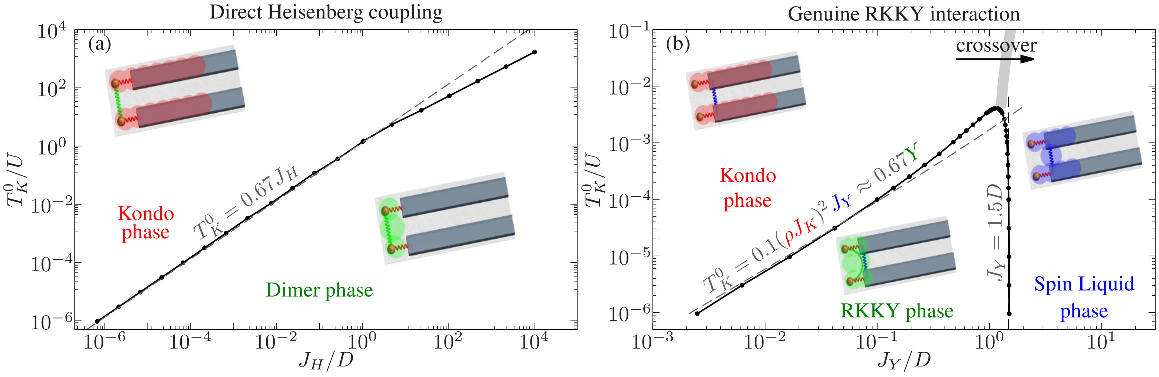

FIG. 2. Phase diagrams of the PH-symmetric 2iA model with (a) direct interimpurity exchange J_{H} and (b) conduction-host-mediated RKKY interaction $Y \approx (\rho J_{\mathrm{K}})^2 J_Y/4$. The black dots mark the QPT positions calculated by NRG, connected by lines for clarity. The dashed lines represent $J_{\mathrm{H}} = 1.5T_{\mathrm{K}}^0$ and $T_{\mathrm{K}}^0 = 1.5Y$, respectively, as indicated. The insets illustrate the spatial structure of the spin correlations in the different phases.

at low energies [35]. Our NRG calculations show that $J_Y^{**} \approx 1.5D$ for metallic leads with rectangular, normalized density of states of width $2D$, $\rho(\omega) = 1/(2D)$. The spin correlations induced by $J_Y > J_Y^{**}$ in the hosts form a spatially extended object of size $\xi_H \approx v_F/J_Y$ (with v_F the Fermi velocity), which we call the *Heisenberg cloud*.

Direct Heisenberg exchange. For comparison below, we now map out the phase diagram of the 2iA model with a direct Heisenberg exchange. This amounts to replacing the last term of the Hamiltonian (1) with the direct impurity coupling term $J_{\mathrm{H}}\vec{S}_1 \cdot \vec{S}_2$. As expected, we find for this PH-symmetric Anderson model the same QPT between a Kondo singlet and a dimer singlet phase as in the JV two-impurity Kondo model [24–26]. It is marked by discontinuous jumps of the impurity and host spectral densities $\mathcal{A}_{T=0}(0), \mathcal{B}_{T=0}(0)$ from 1 to 0 and 0 to 1, respectively, from the Kondo screened phase to the dimer phase. Thus, this constitutes a coupling-decoupling QPT in the charge sector where the Kondo phase is governed by the Kondo QPs described above and the dimer phase by free Bloch electrons. Nevertheless, the impurity and conduction spins remain correlated for all $0 < J_{\mathrm{H}} < \infty$, and static correlations $\langle \vec{S}_1 \cdot \vec{S}_2 \rangle_{T=0}$ are continuous functions of J_{H} through the QPT [25]. In Fig. 2(a) we show the resulting phase diagram in the J_{H}-T_{K}^0 plane near $T = 0$, where $U = D/2$ was used throughout and T_{K}^0 determined from the single-impurity NRG flow for a given parameter set (U, Γ) as described below. In particular, we find the phase transition line as $J_{\mathrm{H}} = 1.5T_{\mathrm{K}}^0$, with slight deviations for $J_{\mathrm{H}}/D \gg 1$, as compared to $J_{\mathrm{H}} = 2.2T_{\mathrm{K}}^0$ for the JV two-impurity Kondo model [25].

RKKY coupling and QSL. We now consider the full 2iA model (1). As can be seen from the discussion of the Heisenberg cloud above, the interhost spin coupling J_Y destabilizes not only the Kondo phase via the RKKY interaction (see below), but also the (almost) free Bloch states in the host towards an interhost spin-correlated phase, when the relevant coupling exceeds the characteristic energy scale of the destabilized phase, i.e., $Y \gtrsim T_{\mathrm{K}}^0$ and $J_Y \gtrsim D$, respectively. We therefore extend our study to large J_Y of the order of the conduction bandwidth D, using $U = D/2$ and $\Gamma = 0.0488U$ corresponding to $T_{\mathrm{K}}^0 \approx 10^{-4}U$, for the numerical evaluations. The temperature dependence of the impurity conductance $G(T)$ and of the host conductance at the impurity site $g(T)$, each normalized to its unitary value, G_0 and g_0, is shown in Figs. 3(a) and 3(b), respectively. It is seen that there exist three stable, low-energy fixed points characterized by the $T = 0$ conductances as

(1) Kondo : $G(0) = G_0,\ g(0) = 0$ (red curves),

(2) RKKY : $G(0) = 0,\ g(0) = g_0$ (green curves),

(3) QSL : $G(0) = \text{fractional},\ g(0) = 0$ (blue curves).

These are attained for different interhost coupling strengths J_Y separated by QPTs at $J_Y = J_Y^*$ (long-dashed curve) and $J_Y = J_Y^{**}$ (short-dashed curve) as shown in the figure. The behaviors in phases (1) and (2) are as in the 2iA model with direct Heisenberg exchange (see above). Phases (1) and (2) are therefore identified with the well-known Kondo and the RKKY (dimer) phases, respectively. The fixed point (3) is strikingly different. First, the fractional value of the impurity conductance $G(0)$ in the most PH-symmetric case appears rather unexpectedly. While for simple Fermi-liquid leads, $G(0)$ would be guaranteed to be either 0 or G_0, the interaction J_Y allows for a very different scenario with $0 < G(0) < G_0$. With the host conductance $g(T) \sim T^2$, this can be understood as a distribution of the scattering phase shift between the impurity and the interacting part of the conduction band, or fractionalization of the (Fermi-liquid) QPs into conduction band and impurity components. Together with the nonlocal spin correlations shown in Fig. 4 and discussed below, these are the defining features of a QSL. The mechanism stabilizing the two-impurity QSL, namely competition between Kondo coupling and intraband spin exchange, does not rely on a small number of impurities and will still be active in bulk systems. Thus, we call phase (3) the two-impurity QSL state or two-impurity analog of a QSL.

An important observation is that each of the $G(T)$ and $g(T)$ curves in Figs. 3(a) and 3(b) is characterized by two temperature scales, $T_{\mathrm{Kw}}(J_Y)$ at which the system flows away from the high-T free-local-moment fixed point, and a strong-coupling scale on which the respective Kondo, RKKY, or QSL strong-coupling fixed points are attained. From the NRG flow, in the Kondo phase ($J_Y < J_Y^*$) we define $T_{\mathrm{Kw}}(J_Y)$ as the temperature where $G_T(0)$ reaches 1/2 of its maximum value G_0, and $T_{\mathrm{Ks}}(J_Y)$ as the temperature where it becomes

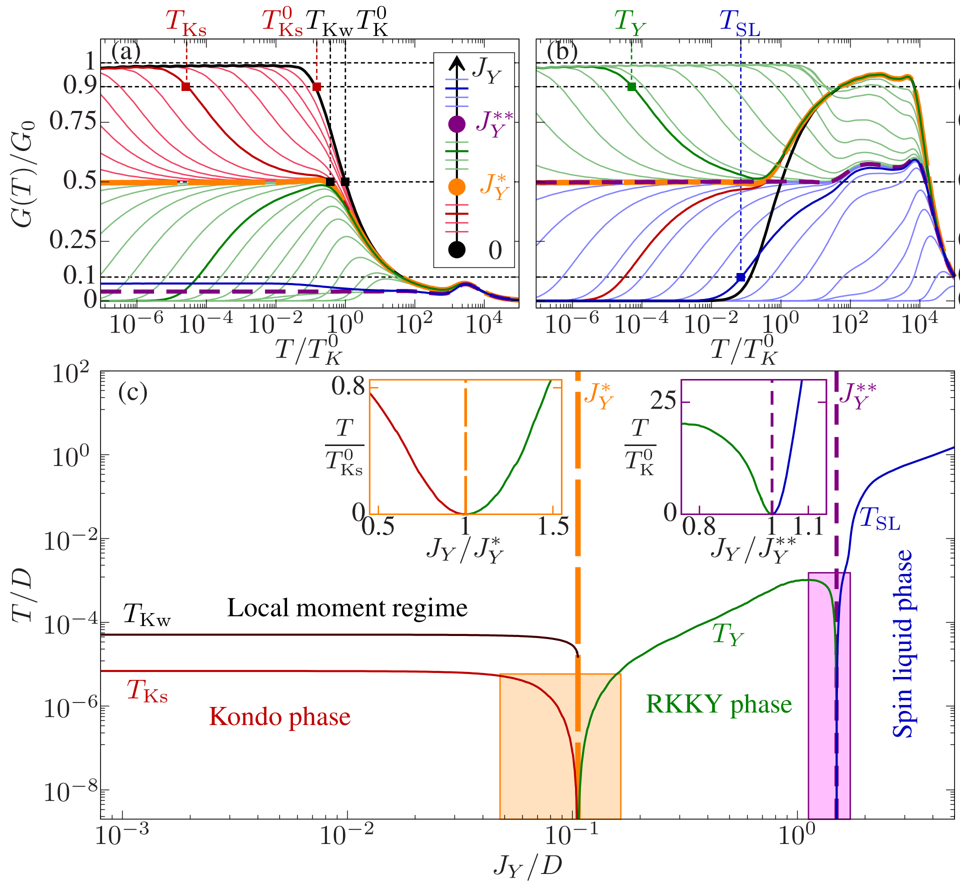

FIG. 3. RG flow and crossover scales in the Kondo, RKKY, and QSL phases. (a) and (b) show the temperature-dependent impurity conductance $G(T)$ and the host conductance at the site of the impurity $g(T)$, respectively. The crossover scales are identified as explained in the text. The long (short) dashed lines were obtained for the quantum critical points at $J_Y = J_Y^*$ ($J_Y = J_Y^{**}$), respectively. (c) The crossover scales $T_{\rm Kw}$, $T_{\rm Ks}$, T_Y, and $T_{\rm SL}$ as a function of J_Y. The insets represent the zoomed-in shaded areas around the QPTs. All computations were done for the parameter values $U/D = 1/2$, $\Gamma/U = 0.0488$, corresponding to $T^0_{\rm K}/U \approx 10^{-4}$.

$G(T) > 0.9G_0$ [cf. Fig. 3(a)]. While for $J_Y = 0$, $T_{\rm Kw}(0)$ coincides with the single-impurity Kondo scale $T^0_{\rm K}$ and is proportional to the strong-coupling scale $T_{\rm Ks}(0)$, $T_{\rm Kw}(J_Y)$ and $T_{\rm Ks}(J_Y)$ are in general independent, depending on two parameters $T^0_{\rm K}$ and J_Y. In the RKKY phase ($J_Y^* < J_Y < J_Y^{**}$), and in the QSL phase ($J_Y > J_Y^{**}$), the respective strong-coupling scales T_Y and $T_{\rm SL}$ are defined as the temperature where $g(T)/g_0 = 0.9$ and $g(T)/g_0 = 0.1$ [cf. Fig. 3(b)]. The dependence of the crossover scales on the RKKY parameter J_Y is shown in Fig. 3(c). We note that all strong-coupling scales vanish quadratically at the respective quantum critical points; see the insets of Fig. 3(c). However, the weak-coupling Kondo scale $T_{\rm Kw}$ remains finite with a suppression factor of $T_{\rm Kw}(J_Y^*)/T^0_{\rm K} \approx 1/e$ (with $e \approx 2.718$ the Euler's constant), and ceases to exist beyond J_Y^*, in agreement with the analytic result of Ref. [35].

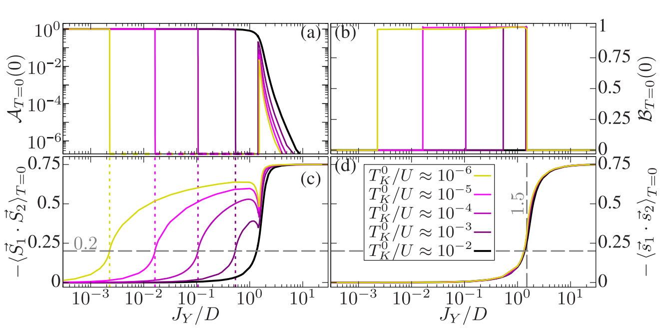

FIG. 4. Signatures of the QPTs in physical quantities, depending on the RKKY coupling parameter J_Y at $T = 0$. (a) and (b) show the normalized impurity and conduction spectral densities, $\mathcal{A}_0(0)$ and $\mathcal{B}_0(0)$, respectively. The static spin correlations between the impurity spins and between the conduction spins at the impurity site are shown in (c) and (d).

The dependence of physical quantities on the RKKY parameter J_Y are shown in Fig. 4 for fixed $T^0_{\rm K}$. For sufficiently low $T^0_{\rm K}$, the quasiparticle spectral densities $\mathcal{A}_0(0) = G(0)$ and $\mathcal{B}_0(0) = g(0)$ exhibit discontinuous jumps signaling the two phase transitions at J_Y^* and J_Y^{**}, respectively. In the QSL phase ($J_Y > J_Y^{**}$), $\mathcal{A}_0(0)$ has fractional values which decay to zero into the QSL phase. This signals incomplete (and deep in the QSL phase vanishing) Kondo screening of the impurity spins. The static impurity-spin correlations [Fig. 4(c)] behave continuously at the Kondo-to-RKKY transition, as expected from a JV-like QPT, but exhibit a sharp cusp at the RKKY-to-QSL QPT and approach the singlet value of $-3/4$ deep in the QSL phase. By contrast, the conduction spin correlations [Fig. 4(d)] show no indication of singular behavior. The fact that anomalous behavior appears only in the impurity (fractional charge excitations and spin correlations) but not in the conduction electron sector, gives rise to defining this phase as a two-impurity analog of a quantum spin liquid. Above a critical value of T_K^0 (i.e., for sufficiently strong Kondo coupling) all quantities behave continuously, i.e., there exists no QPT (see curves for $T_K^0 \approx 10^{-2}U$ in Fig. 4).

All these results can now be summarized in the complete phase diagram of the RKKY 2iA model Eq. (1) shown in Fig. 2(b). While the Kondo-to-RKKY QPT is essentially identical to the one of the model with direct Heisenberg exchange [Fig. 2(a)] with a critical line of $Y \approx 1.5T_K^0$, the RKKY-to-QSL line is independent of T_K^0 and occurs at a large coupling of $J_Y \approx 1.5D$. This is expected, because the couplings Y and J_Y destabilize the quasiparticles in the Kondo and in the RKKY phases at their respective characteristic energy scales, T_K^0 and D. The independence of the RKKY-to-QSL transition line of T_K^0 implies that it must meet with the Kondo-to-RKKY transition line. That is, the RKKY phase must terminate at a critical value of T_K^0, as seen in Fig. 2(b), and the zero-temperature QSL and Kondo phases are continuously connected via a crossover at large T_K^0. Note that this is in stark contrast to the case of a direct Heisenberg interaction between the impurities [Fig. 2(a)], where the QPT exists for all values of T_K^0.

Conclusion and experimental realization. We report the detection of a new, stable fixed point, exhibiting quantum spin-liquid features in a model of two magnetic ions coupled to a metallic electron system with additional spin coupling within the conduction band. This phase is characterized by nonlocal spin entanglement and fractionalized charge excitations on the magnetic ions, an analog of spin liquids in lattice systems. This quantum spin liquid is stabilized by a dynamical frustration effect, i.e., the interplay of Kondo spin screening and strong conduction-electron spin correlations with a correlation energy of the order of the conduction bandwidth. Geometrical frustration is not required, but may enhance the effect, in particular, reduce the critical intraband correlation strength for the formation of the spin-liquid phase. In heavy-fermion compounds or Anderson lattice systems, such correlations may be achieved near a magnetic, e.g., spin-density-wave instability within the conduction electron system. This phase may also be realized experimentally in two-impurity systems with a low conduction bandwidth, such as magic-angle bilayer graphene [41], with magnetic coupling between the layers.

Acknowledgments. Stimulating discussions with Frithjof Anders, Fabian Eickhoff, Andreas Gleis, Mohsen Hafez-Torbati, and Kacper Wrześniewski are gratefully acknowledged. This project was financially supported by the Deutsche Forschungsgemeinschaft (DFG, German Research Foundation) under Germany's Excellence Strategy – Cluster of Excellence *Matter and Light for Quantum Computing*, ML4Q (390534769), and through the DFG Collaborative Research Center CRC 185 OSCAR (277625399). K.P.W. acknowledges funding by the Alexander von Humboldt Foundation and support from the Polish National Science Centre through Grant No. 2018/29/B/ST3/00937.

[1] P. Anderson, Resonating valence bonds: A new kind of insulator? Mater. Res. Bull. **8**, 153 (1973).

[2] P. W. Anderson, The resonating valence bond state in La_2CuO_4 and superconductivity, Science **235**, 1196 (1987).

[3] M. R. Norman, Colloquium: Herbertsmithite and the search for the quantum spin liquid, Rev. Mod. Phys. **88**, 041002 (2016).

[4] L. Savary and L. Balents, Quantum spin liquids: A review, Rep. Prog. Phys. **80**, 016502 (2017).

[5] H. Takagi, T. Takayama, G. Jackeli, G. Khaliullin, and S. Nagler, Concept and realization of Kitaev quantum spin liquids, Nat. Rev. Phys. **1**, 264 (2019).

[6] N. Read and S. Sachdev, Large-*N* Expansion for Frustrated Quantum Antiferromagnets, Phys. Rev. Lett. **66**, 1773 (1991).

[7] H. v. Löhneysen, A. Rosch, M. Vojta, and P. Wölfle, Fermi-liquid instabilities at magnetic quantum phase transitions, Rev. Mod. Phys. **79**, 1015 (2007).

[8] S. Paschen and Q. Si, Quantum phases driven by strong correlations, Nat. Rev. Phys. **3**, 9 (2021).

[9] J. Kondo, Resistance minimum in dilute magnetic alloys, Prog. Theor. Phys. **32**, 37 (1964).

[10] A. C. Hewson, *The Kondo Problem to Heavy Fermions* (Cambridge University Press, Cambridge, UK, 1997).

[11] M. A. Ruderman and C. Kittel, Indirect exchange coupling of nuclear magnetic moments by conduction electrons, Phys. Rev. **96**, 99 (1954).

[12] T. Kasuya, A theory of metallic ferro- and antiferromagnetism on Zener's model, Prog. Theor. Phys. **16**, 45 (1956).

[13] K. Yosida, Magnetic properties of Cu-Mn alloys, Phys. Rev. **106**, 893 (1957).

[14] N. Andrei and P. Coleman, Cooper Instability in the Presence of a Spin Liquid, Phys. Rev. Lett. **62**, 595 (1989).

[15] P. Coleman and N. Andrei, Kondo-stabilised spin liquids and heavy fermion superconductivity, J. Phys.: Condens. Matter **1**, 4057 (1989).

[16] S. Nakatsuji, Y. Machida, Y. Maeno, T. Tayama, T. Sakakibara, J. van Duijn, L. Balicas, J. N. Millican, R. T. Macaluso, and J. Y. Chan, Metallic Spin-Liquid Behavior of the Geometrically Frustrated Kondo Lattice $Pr_2Ir_2O_7$, Phys. Rev. Lett. **96**, 087204 (2006).

[17] S. Lucas, K. Grube, C.-L. Huang, A. Sakai, S. Wunderlich, E. L. Green, J. Wosnitza, V. Fritsch, P. Gegenwart, O. Stockert, and H. v. Löhneysen, Entropy Evolution in the Magnetic Phases of Partially Frustrated CePdAl, Phys. Rev. Lett. **118**, 107204 (2017).

[18] H. Zhao, J. Zhang, M. Lyu, S. Bachus, Y. Tokiwa, P. Gegenwart, S. Zhang, J. Cheng, Y.-f. Yang, G. Chen, Y. Isikawa, Q. Si, F. Steglich, and P. Sun, Quantum-critical phase from frustrated magnetism in a strongly correlated metal, Nat. Phys. **15**, 1261 (2019).

[19] M. Majumder, R. Gupta, H. Luetkens, R. Khasanov, O. Stockert, P. Gegenwart, and V. Fritsch, Spin-liquid signatures in the quantum critical regime of pressurized CePdAl, Phys. Rev. B **105**, L180402 (2022).

[20] R. Tripathi, D. T. Adroja, C. Ritter, S. Sharma, C. Yang, A. D. Hillier, M. M. Koza, F. Demmel, A. Sundaresan, S. Langridge, W. Higemoto, T. U. Ito, A. M. Strydom, G. B. G. Stenning, A. Bhattacharyya, D. Keen, H. C. Walker, R. S. Perry, F. Pratt, Q. Si *et al.*, Quantum critical spin-liquid-like behavior in the $S = \frac{1}{2}$ quasikagome-lattice compound $CeRh_{1-x}Pd_xSn$ investigated using muon spin relaxation and neutron scattering, Phys. Rev. B **106**, 064436 (2022).

[21] K. G. Wilson, The renormalization group: Critical phenomena and the Kondo problem, Rev. Mod. Phys. **47**, 773 (1975).

[22] R. Bulla, T. A. Costi, and T. Pruschke, Numerical renormalization group method for quantum impurity systems, Rev. Mod. Phys. **80**, 395 (2008).

[23] O. Legeza, C. P. Moca, A. I. Toth, I. Weymann, and G. Zarand, Manual for the flexible DM-NRG code, arXiv:0809.3143. The code is available at http://www.phy.bme.hu/~dmnrg/.

[24] B. A. Jones and C. M. Varma, Study of Two Magnetic Impurities in a Fermi Gas, Phys. Rev. Lett. **58**, 843 (1987).

[25] B. A. Jones, C. M. Varma, and J. W. Wilkins, Low-Temperature Properties of the Two-Impurity Kondo Hamiltonian, Phys. Rev. Lett. **61**, 125 (1988).

[26] B. A. Jones and C. M. Varma, Critical point in the solution of the two magnetic impurity problem, Phys. Rev. B **40**, 324 (1989).

[27] R. M. Fye, "Anomalous Fixed Point Behavior" of Two Kondo Impurities: A Reexamination, Phys. Rev. Lett. **72**, 916 (1994).

[28] I. Affleck, A. W. W. Ludwig, and B. A. Jones, Conformal-field-theory approach to the two-impurity Kondo problem: Comparison with numerical renormalization-group results, Phys. Rev. B **52**, 9528 (1995).

[29] F. Eickhoff, B. Lechtenberg, and F. B. Anders, Effective low-energy description of the two-impurity Anderson model: RKKY interaction and quantum criticality, Phys. Rev. B **98**, 115103 (2018).

[30] A. K. Mitchell, P. G. Derry, and D. E. Logan, Multiple magnetic impurities on surfaces: Scattering and quasiparticle interference, Phys. Rev. B **91**, 235127 (2015).

[31] A. K. Mitchell and R. Bulla, Validity of the local self-energy approximation: Application to coupled quantum impurities, Phys. Rev. B **92**, 155101 (2015).

[32] G. Zaránd, C.-H. Chung, P. Simon, and M. Vojta, Quantum Criticality in a Double-Quantum-Dot System, Phys. Rev. Lett. **97**, 166802 (2006).

[33] A. Gleis, S.-S. B. Lee, A. Weichselbaum, G. Kotliar, and J. von Delft (unpublished).

[34] J. Bork, Y.-h. Zhang, L. Diekhöner, L. Borda, P. Simon, J. Kroha, P. Wahl, and K. Kern, A tunable two-impurity Kondo system in an atomic point contact, Nat. Phys. **7**, 901 (2011).

[35] A. Nejati, K. Ballmann, and J. Kroha, Kondo Destruction in RKKY-Coupled Kondo Lattice and Multi-Impurity Systems, Phys. Rev. Lett. **118**, 117204 (2017).

[36] K. P. Wójcik and J. Kroha, Asymmetry effects on the phases of RKKY-coupled two-impurity Kondo systems, Phys. Rev. B **107**, 125146 (2023).

[37] A. Weichselbaum and J. von Delft, Sum-Rule Conserving Spectral Functions from the Numerical Renormalization Group, Phys. Rev. Lett. **99**, 076402 (2007).

[38] F. B. Anders and A. Schiller, Real-Time Dynamics in Quantum-Impurity Systems: A Time-Dependent Numerical Renormalization-Group Approach, Phys. Rev. Lett. **95**, 196801 (2005).

[39] P. Simon and I. Affleck, Finite-Size Effects in Conductance Measurements on Quantum Dots, Phys. Rev. Lett. **89**, 206602 (2002).

[40] L. Borda, Kondo screening cloud in a one-dimensional wire: Numerical renormalization group study, Phys. Rev. B **75**, 041307(R) (2007).

[41] R. Bistritzer and A. H. MacDonald, Moiré bands in twisted double-layer graphene, Proc. Natl. Acad. Sci. USA **108**, 12233 (2011).